

AFCRL - 72-0071

# DAMAGE THRESHOLD STUDIES IN LASER CRYSTALS:

## SURFACE DAMAGE, PREVENTION OF SELF-FOCUSING

By

Concetto R. Giuliano  
Robert W. Hellwarth  
Gerald R. Rickel

HUGHES RESEARCH LABORATORIES  
HUGHES AIRCRAFT COMPANY  
3011 Malibu Canyon Road  
Malibu, California 90265

Contract F19628-69-C-0277  
Project 8693

SEMIANNUAL REPORT 5  
JANUARY 1972



APPROVED FOR PUBLIC RELEASE; DISTRIBUTION UNLIMITED.

Contract Monitor: Erlan S. Bliss, Capt., USAF  
OPTICAL PHYSICS LABORATORY

Sponsored by  
Advanced Research Projects Agency  
ARPA Order 1434  
Monitored by  
AIR FORCE CAMBRIDGE RESEARCH LABORATORIES  
AIR FORCE SYSTEMS COMMAND  
UNITED STATES AIR FORCE  
BEDFORD, MASSACHUSETTS 01730

AD 740487

Program Code No. . . . . 9D10  
 Effective Date of Contract . . . . . 21 May 1969  
 Contract Expiration Date . . . . . 15 July 1972  
 Principal Investigator . . . . . Concetto R. Giuliano  
 (213)456-6411, ext. 208  
 Project Scientist or Engineer . . . . Erlan S. Bliss, Capt. USAF  
 (617)861-2600

ACCESSION for		
CFSTI	WHITE SECTION	<input checked="checked" type="checkbox"/>
DCC	BUFF SECTION	<input type="checkbox"/>
SWAN.	CED.	<input type="checkbox"/>
JUSTIFICATION .....		
BY .....		
DISTRIBUTION/AVAILABILITY CODES		
DIST.	AVAIL. and/or SPECIAL	
<b>A</b>		

Qualified requestors may obtain additional copies from the  
 Defense Documentation Center. All others should apply to  
 the National Technical Information Service.

UNCLASSIFIED

Security Classification

## DOCUMENT CONTROL DATA - R&amp;D

(Security classification of title, body of abstract and indexing annotation must be entered when the overall report is classified)

1. ORIGINATING ACTIVITY (Corporate author) Hughes Research Laboratories 3011 Malibu Canyon Road Malibu, California 90265	2a. REPORT SECURITY CLASSIFICATION Unclassified
	2b. GROUP

3. REPORT TITLE  DAMAGE THRESHOLD STUDIES IN LASER CRYSTALS: SURFACE DAMAGE, PREVENTION OF SELF-FOCUSING
---

4. DESCRIPTIVE NOTES (Type of report and inclusive dates) Scientific. Interim
--

5. AUTHOR(S) (First name, middle initial, last name) Concetto R. Giuliano Robert W. Hellwarth Gerald R. Rickel
---

6. REPORT DATE January 1972	7a. TOTAL NO. OF PAGES 42	7b. NO. OF REFS 5
--------------------------------	------------------------------	----------------------

8a. CONTRACT OR GRANT NO. Arpa Order 1434 F19628-69-C-0277	9a. ORIGINATOR'S REPORT NUMBER(S)
---	-----------------------------------

b. PROJECT, TASK, WORK UNIT NOS. 8693 N/A N/A	9b. OTHER REPORT NO(S) (Any other numbers that may be assigned this report)  AFCRL-72-0071
--	--

c. DOD ELEMENT 61101D	
--------------------------	--

d. DOD SUBELEMENT N/A	
-----------------------	--

10. DISTRIBUTION STATEMENT  Approved for public release; distribution unlimited. (A)
--

11. SUPPLEMENTARY NOTES This research was supported by the Advanced Research Projects Agency.	12. SPONSORING MILITARY ACTIVITY Air Force Cambridge Research Laboratories (OP) L.G. Hanscom Field Bedford, Massachusetts 01730
--	--

13. ABSTRACT <p>In this report initial experimental results on laser induced surface damage are discussed. The dependence of surface damage threshold on the distance between the focusing lens and sample indicates that surface damage for sapphire is a power density phenomenon. It is also pointed out that the exit surface damage threshold for sapphire is not connected with any nonlinear processes taking place deep within the bulk of the material, such as self-focusing. The possibility that bulk phenomena might affect the exit damage threshold for ruby cannot be eliminated at this time. The relationship between surface plasmas and surface damage was also studied. Streak camera experiments in which the temporal evolution of the plasmas was observed and other experiments in which the sample surface was tilted with respect to the incident light beam indicate that the surface plasma is a result of, rather than a cause of, the damage. It is also observed that the plasmas grow away from the surfaces with time, contrary to a previously reported result which postulated in an attempt to explain the difference between entrance and exit damage that both entrance and exit plasmas grow toward the laser. It was also found that the entrance plasma has two components, one of which appears to arise from a surface explosion and the other which is an air plasma sustained directly by the laser beam; the exit plasma has one component - the surface explosion type. Results of the effect of ion beam polishing on surface damage threshold show that, in spite of large fluctuations in the data, improvements of as much as a factor of seven can be obtained over conventional abrasive polishing. The effect of beam shape on self-focusing damage is also discussed. It is shown that the self-focusing threshold for elliptical beams is higher than that for circular beams, increasing linearly as the aspect ratio for large aspect ratios. The implications of these results are very important because they indicate that self-focusing can be avoided by choice of the appropriate beam shape. Theoretical considerations in this report have been concentrated mainly on a further pursuit of the question of whether optical breakdown does or does not involve an avalanche of hot electrons and also a consideration of means of measuring surface absorption at the faces of crystals so that the role of this absorption in surface damage may be assessed.</p>
--

UNCLASSIFIED

Security Classification

14. KEY WORDS	LINK A		LINK B		LINK C	
	ROLE	WT	ROLE	WT	ROLE	WT
Surface Damage						
Surface Plasmas						
Entrance and Exit Damage						
Damage Thresholds						
Streak Camera Experiments						
Ion Beam Polishing						
Sapphire						
Ruby						
Self-Focusing						
Noncircular Beams						

UNCLASSIFIED

Security Classification

AFCRL-72-0071

DAMAGE THRESHOLD STUDIES IN LASER CRYSTALS:  
Surface Damage, Prevention of Self-Focusing

by

Concetto R. Giuliano  
Robert W. Hellwarth  
Gerald R. Rickel

HUGHES RESEARCH LABORATORIES  
*a division of hughes aircraft company*  
Malibu, California 90265

Contract F19628-69-C-0277  
Project 8693

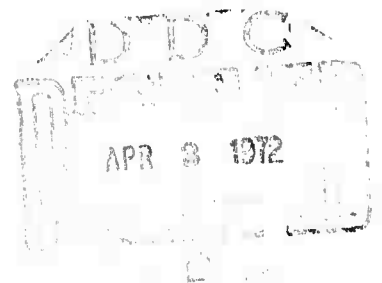
Semiannual Report 5

Details of illustrations in  
this document may be better  
studied on microfiche

Contract Monitor: Erlan S. Bliss, Capt., USAF  
Optical Physics Laboratory

*Sponsored by*  
Advanced Research Projects Agency  
ARPA Order 1434

*Monitored by*  
AIR FORCE CAMBRIDGE RESEARCH LABORATORIES  
AIR FORCE SYSTEMS COMMAND  
UNITED STATES AIR FORCE  
Bedford, Massachusetts 01730



Approved for public release; distribution unlimited.

## ABSTRACT

In this report initial experimental results on laser induced surface damage are discussed. The dependence of surface damage threshold on the distance between the focusing lens and sample indicates that surface damage for sapphire is a power density phenomenon. It is also pointed out that the exit surface damage threshold for sapphire is not connected with any nonlinear processes taking place deep within the bulk of the material, such as self-focusing. The possibility that bulk phenomena might affect the exit damage threshold for ruby cannot be eliminated at this time. The relationship between surface plasmas and surface damage was also studied. Streak camera experiments in which the temporal evolution of the plasmas was observed and other experiments in which the sample surface was tilted with respect to the incident light beam indicate that the surface plasma is a result of, rather than a cause of, the damage. It is also observed that the plasmas grow away from the surfaces with time, contrary to a previously reported result which postulated in an attempt to explain the difference between entrance and exit damage that both entrance and exit plasmas grow toward the laser. It was also found that the entrance plasma has two components, one of which appears to arise from a surface explosion and the other which is an air plasma sustained directly by the laser beam; the exit plasma has one component - the surface explosion type. Results of the effect of ion beam polishing on surface damage threshold show that, in spite of large fluctuations in the data, improvements of as much as a factor of seven can be obtained over conventional abrasive polishing. The effect of beam shape on self-focusing damage is also

discussed. It is shown that the self-focusing threshold for elliptical beams is higher than that for circular beams, increasing linearly as the aspect ratio for large aspect ratios. The implications of these results are very important because they indicate that self-focusing can be avoided by choice of the appropriate beam shape. Theoretical considerations in this report have been concentrated mainly on a further pursuit of the question of whether optical breakdown does or does not involve an avalanche of hot electrons and also a consideration of means of measuring surface absorption at the faces of crystals so that the role of this absorption in surface damage may be assessed.

## TABLE OF CONTENTS

	ABSTRACT . . . . .	<i>iii</i>
	LIST OF ILLUSTRATIONS . . . . .	<i>vii</i>
I	EXPERIMENTAL STUDIES ON OPTICAL DAMAGE . . . . .	1
	A. Introduction and Summary of Results . . . . .	1
	B. Damage Threshold as a Function of Beam Size and Divergence . . . . .	2
	C. Relationship Between Surface Damage and Plasma Formation . . . . .	6
	D. Effect of Ion Beam Polishing on Surface Damage . . . . .	23
	E. Bulk Damage and Self-Focusing for Noncircular Beams . . . . .	27
II	THEORETICAL STUDIES ON OPTICAL DAMAGE . . . . .	31
	A. Mechanisms of Optical Breakdown . . . . .	31
	B. Means of Measuring Surface Absorption . . . . .	33
III	PLANS FOR NEXT PERIOD . . . . .	37
	REFERENCES . . . . .	39
	DD FORM 1473 . . . . .	41



## LIST OF ILLUSTRATIONS

Fig. 1.	Exit surface damage threshold power for sapphire and ruby samples as a function of surface distance from beam waist for 19 cm lens . . . . .	4
Fig. 2.	Beam area and entrance surface damage threshold as a function of surface distance from beam waist for 19 cm lens . . . . .	5
Fig. 3.	Photographs of entrance surface plasma on sapphire for different amounts of optical attenuation between camera and sample . . . . .	8
Fig. 4.	Photographs of exit surface plasma on sapphire for different amounts of optical attenuation between camera and sample . . . . .	9
Fig. 5.	Schematic diagram showing setup used for photographing surface plasmas both for still and streak photography . . . . .	11
Fig. 6.	Streak photograph of entrance plasma on sapphire surface showing two temporal components . . . . .	14
Fig. 7.	Streak photograph of exit plasma on sapphire surface . . . . .	14
Fig. 8.	Time integrated photographs of entrance plasma at sapphire surface tilted with respect to incident beam direction . . . . .	17
Fig. 9.	Time integrated photograph of exit plasma at sapphire surface tilted 45° with respect to light propagation direction . . . . .	18

Fig. 10.	Time integrated photographs of entrance plasma at sapphire surface tilted $26^\circ$ from beam direction for different optical attenuations at camera . . . . .	19
Fig. 11.	Streak photographs of entrance plasma as viewed through different interference filters . . . . .	22

## SECTION I

### EXPERIMENTAL STUDIES ON OPTICAL DAMAGE

#### A. INTRODUCTION AND SUMMARY OF RESULTS

The main emphasis of the experimental effort in this reporting period has been placed on the phenomenon of surface damage. Section I-B describes the results of experiments on ruby and sapphire in which the lens-to-sample distance was varied so that the surface was subjected to a series of different spot sizes for both diverging and converging beams. The results for sapphire show that the surface damage has a power density dependence and indicate that the damage mechanism is strictly a surface or near-surface phenomenon. The results for ruby are more complicated and appear to be related to a power dependent beam distortion effect, as described in an earlier report. Section I-C discusses the results of experiments which were designed to determine the relationship between the surface damage and the plasmas that are seen to accompany the damage. A series of observations indicates that the plasmas are a result of the damage rather than a cause of the damage. These experiments include streak camera studies in which the temporal evolution of both entrance and exit plasmas was observed. Other photographic observations of plasmas formed at surfaces tilted with respect to the light beam combined with the streak camera studies yield the conclusion that the exit plasma results from a microexplosion at the surface while the entrance plasma contains two components, one of which appears to be an

air plasma and the other an explosion plasma similar to that at the exit surface. Section I-D contains a few preliminary results of the ion beam polishing effect on increasing surface damage threshold. In spite of the fact that a great deal of fluctuation exists in the data, these results indicate the importance of surface finish on damage resistance. Section I-E is a discussion of the phenomenon of bulk damage and self-focusing for beams of noncircular cross-section, indicating that the self-focusing threshold and hence bulk damage threshold for beams of elliptical cross-section increases linearly as the aspect ratio and therefore is least for circular beams. This result is semiquantitatively supported by a few damage experiments performed with noncircular beams. The implications of these results are very significant because they indicate that any difficulties in a system which might arise from self-focusing can be avoided by choosing the appropriate beam shape.

#### B. DAMAGE THRESHOLD AS A FUNCTION OF BEAM SIZE AND DIVERGENCE

One of the questions which arose in the consideration of exit surface damage was concerned with the possibility that the damage at the exit surface might be influenced by what the beam does in the bulk of the material. For example, if some self-focusing takes place, it might affect the beam so that the intensity at the exit face will be different from that expected. Also, some phenomenon which might cause the generation of acoustic waves directed toward the exit surface would be affected by how the beam propagates inside the sample before reaching the exit surface. A series of experiments on sapphire and ruby was carried out in which

the sample was moved relative to the focusing lens, so that the spot size at the surface would vary over a wide range and also so that the beam could be either converging or diverging at the surface depending on whether the beam waist lay downstream or upstream from the surface.

The result of these experiments are shown in Fig. 1. In these experiments a 19 cm lens for focusing the light from the mode controlled ruby laser (described in the earlier reports) was used. The ruby and sapphire samples were moved in 5 mm increments relative to the lens, and surface damage threshold was measured for each location. The data on the left half of Fig. 1 correspond to the case of rays converging at the surface and the data on the right half to diverging rays. The beam area is also plotted as a function of distance in the figure, the solid line showing the beam area calculated on the basis of the mode propagation equations described in Semiannual Report No. 1 and the dashed line showing the result of our measurements of beam size near the waist described in Semiannual Report No. 3.

Figure 1 shows that the results for exit surface damage threshold power in sapphire sample L134 fall very close to the beam area curve. The fact that they fall so closely is a coincidence of the scale and the units chosen, but the fact that they have the same functional dependence on distance is significant in that it strongly indicates that the damage threshold is a power density phenomenon. Also, the fact that the threshold is independent of whether the beam is converging or diverging at the exit surface indicates that the damage seems to be strictly a surface or near-surface phenomenon. The exit surface damage threshold for this sample is about  $1 \text{ GW/cm}^2$ . The data for entrance surface

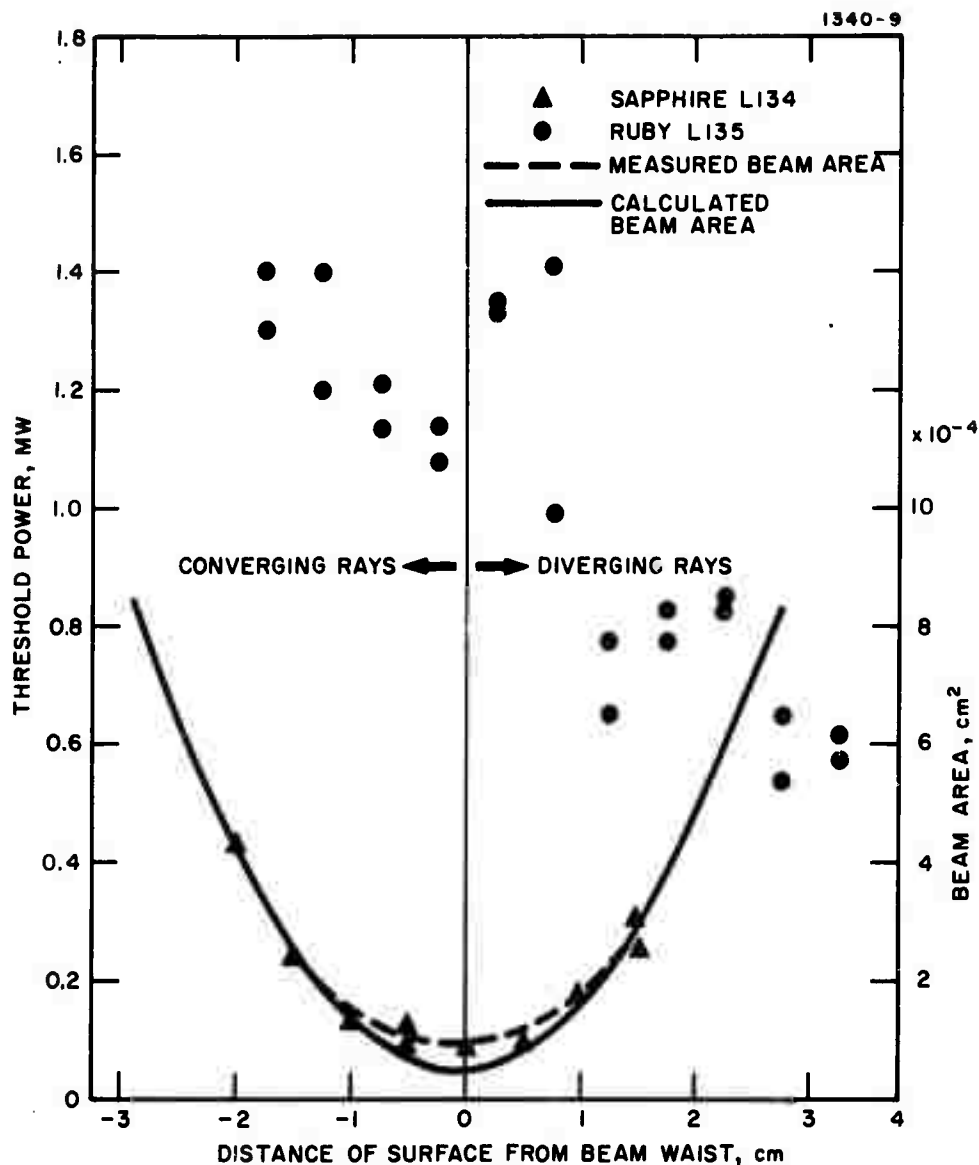


Fig. 1. Exit surface damage threshold power for sapphire and ruby samples as a function of surface distance from beam waist for 19 cm lens. Beam area is also plotted. The left half of the figure corresponds to a converging beam; the right half to a diverging beam.

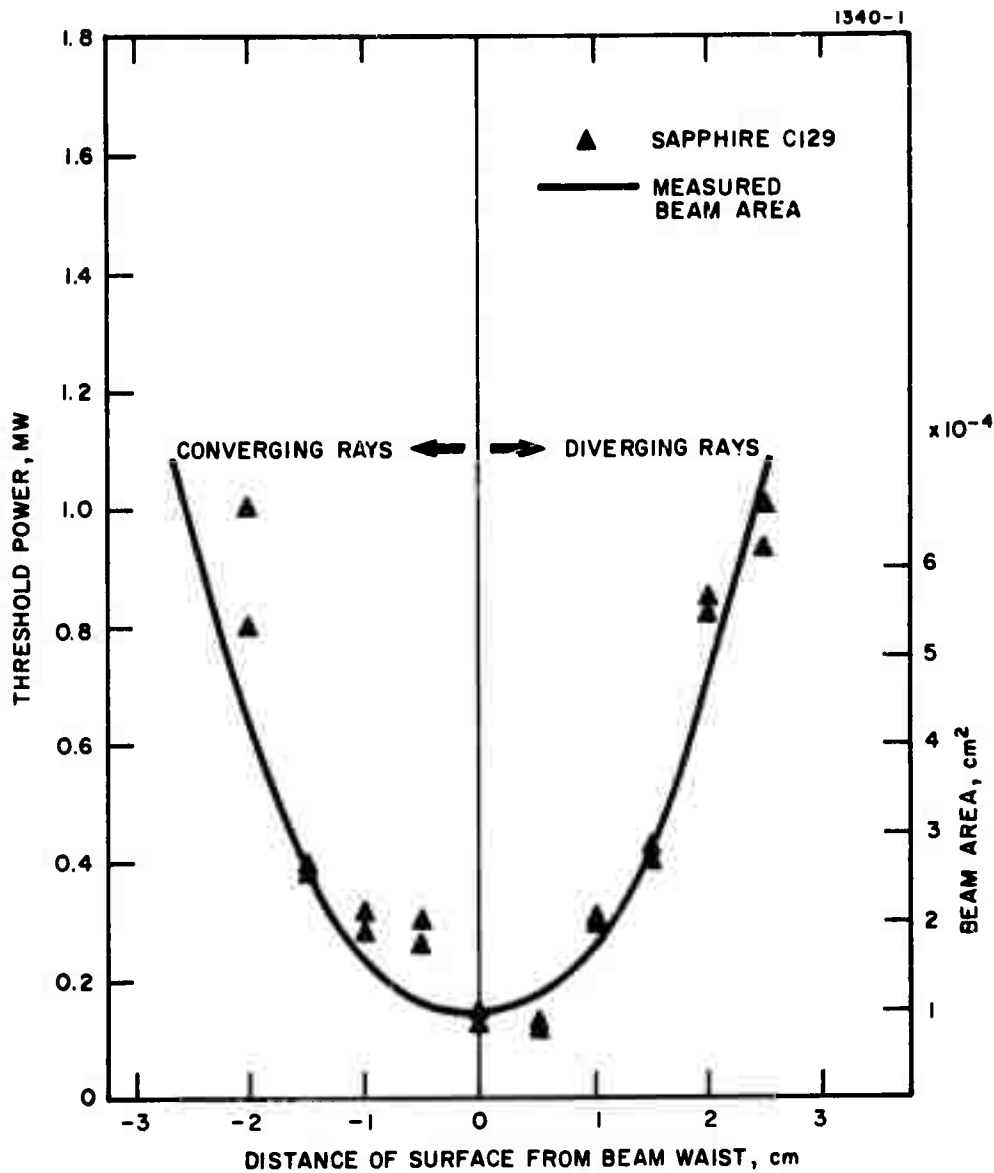


Fig. 2. Beam area and entrance surface damage threshold as a function of surface distance from beam waist for 19 cm lens.

damage for sapphire sample C129 have a similar dependence on lens to sample distance, but in this case the scatter in the points is somewhat greater. These results are shown in Fig. 2. Here the beam area curve is plotted on a different scale than in Fig. 1 to show that the dependence of threshold power with distance is essentially the same as the dependence of beam area with distance. The entrance damage threshold for this case is about  $1.5 \text{ GW/cm}^2$ .

The dependence of exit damage threshold power with lens to sample distance for ruby sample L135 is also shown in Fig. 1. A very different behavior than for sapphire is also shown in this figure. Semiannual Report No. 3 reported the observation of a power dependent beam distortion in ruby where the beam profile was seen to deviate severely from the incident gaussian profile. The beam profile showed bright spots and on-axis minima, which varied with the incident power over a range that was well below the damage threshold. This phenomenon, which was not observed in sapphire, is not understood but may be related to the ruby absorption at  $6943 \text{ \AA}$ . The fact that the beam profile in ruby changes with incident power and position indicates that the power density at a given location (e.g., the exit surface) cannot be easily determined. The data in Fig. 1 for ruby appear to be another manifestation of this beam distortion.

### C. RELATIONSHIP BETWEEN SURFACE DAMAGE AND PLASMA FORMATION

During this reporting period, much emphasis has been placed on study of the surface plasmas and their possible connection with surface damage. It has been the observation of various workers that each time a plasma occurs, surface damage also occurs. In fact, the occurrence of a plasma has



been held to be a criterion for surface damage. From this has followed the suggestion that the surface plasma might be causing surface damage.<sup>1</sup> The difference between the appearance of entrance and exit damage might be explained by the motion of the plasma in its growth relative to the surface.

A number of experiments were devised and carried out to answer the following questions:

- Does a plasma always accompany surface damage?
- If so, does the plasma cause the damage or does it result from it, or does it merely accompany it, having no real connection with the damage?

The answers to the above questions, plus further details concerning the plasma development and behavior, promise to provide additional insight into the nature of surface damage and to a solution of the problem.

#### 1. Entrance and Exit Plasmas

In Semiannual Report No. 2, brief mention was given to the fact that the exit and entrance damage plasmas are different in physical appearance, the entrance plasma being rounded and the exit plasma more pointed. More careful examination of these plasmas at high magnification shows other features that were not apparent on first observation. Figures 3 and 4 show photographs of entrance and exit plasmas for sapphire taken at varying exposures. It is seen in Figs. 3(a) and 4(a) that the rounded and pointed features are presented in the entrance and exit plasmas, respectively. These photographs are, however, highly overexposed. Parts (b), (c), and (d) of Figs. 3 and 4 show the surface plasmas with different amounts of optical attenuation between the camera and the

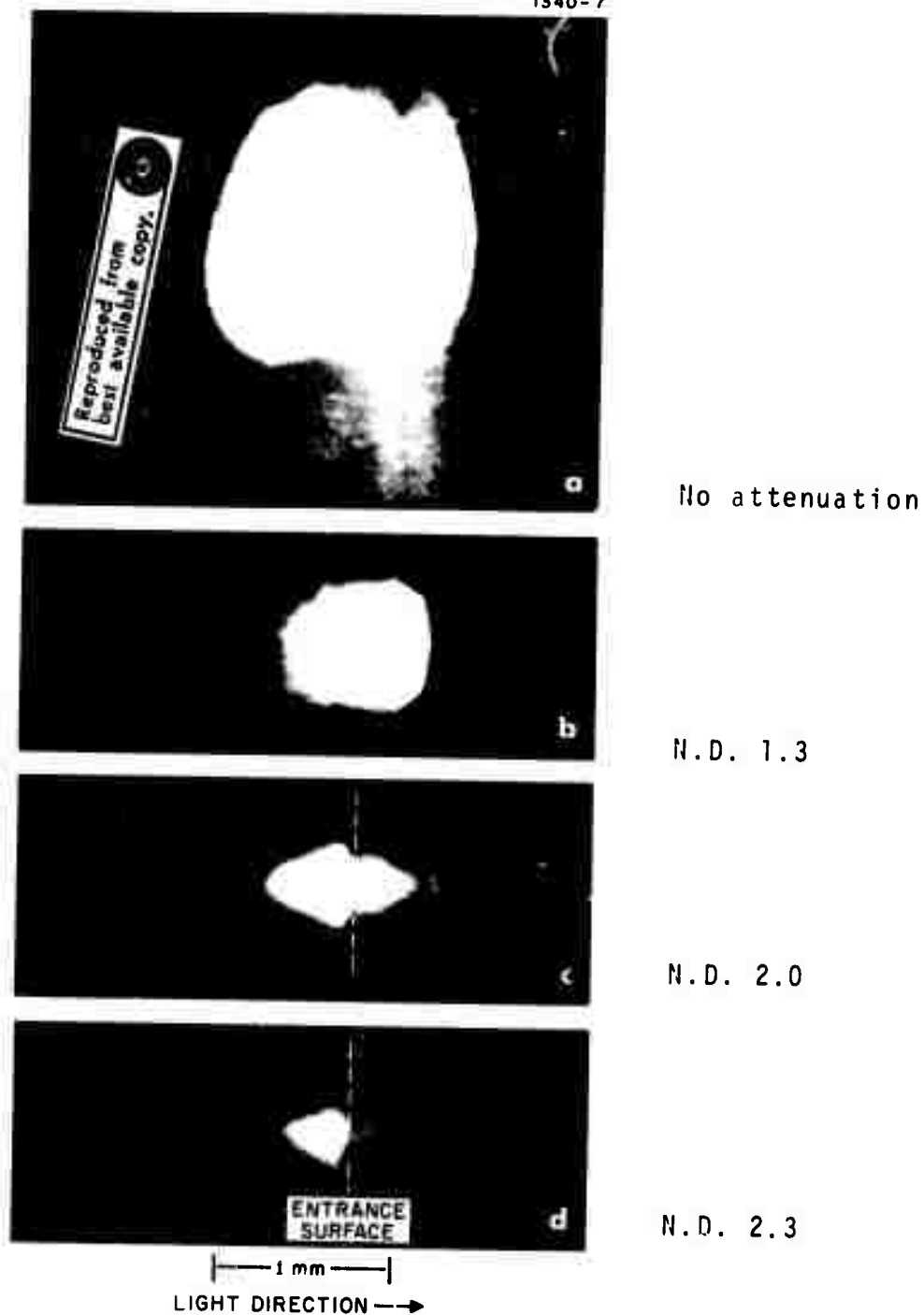


Fig. 3. Photographs of entrance surface plasma on sapphire for different amounts of optical attenuation between camera and sample.



No attenuation



N.D. 0.7



N.D. 1.3



N.D. 1.7

1 mm  
LIGHT DIRECTION →

Reproduced from  
best available copy.



Fig. 4. Photographs of exit surface plasma on sapphire for different amounts of optical attenuation between camera and sample.

sample. The setup used to obtain these photographs is shown in Fig. 5. The unamplified output from the ruby laser ( $TEM_{00}$ , 1 MW, 20 nsec FWHM) was focused to a 55  $\mu\text{m}$  spot on either the entrance or exit surface using a 19 cm lens. Thus the power density in these experiments ( $\sim 10 \text{ GW/cm}^2$ ) is about ten times the surface damage threshold. The pictures of the surface plasmas with less exposure show different qualitative features than the overexposed photographs. These photographs are included for completeness but an interpretation of them will not be offered in this report.

Because the photographic setup is such that the camera views the surface at an angle less than  $90^\circ$  to the normal (see Fig. 5), both the plasma and its reflection in the surface are often seen. Evidence of this reflection is seen in almost all the photographs shown in this section. The fact that there are indeed reflections was confirmed by placing an appropriately oriented Polaroid filter in front of the camera, in which case the reflection from the dielectric surface disappeared as expected.

## 2. Surface Damage Without Plasma Formation

We have carried out a few experiments in which surface damage was generated without observing an accompanying plasma. These experiments were conducted on sapphire samples and applied only to the exit surface (entrance damage was not pursued in this series of experiments). In these experiments we observed the exit surface during laser irradiation both visually and photographically under different conditions of optical filtering and exposure. It was found that when the sample was exposed to focused radiation very close to threshold, damage could be generated in the form of a series of micropits without the simultaneous accompaniment of a

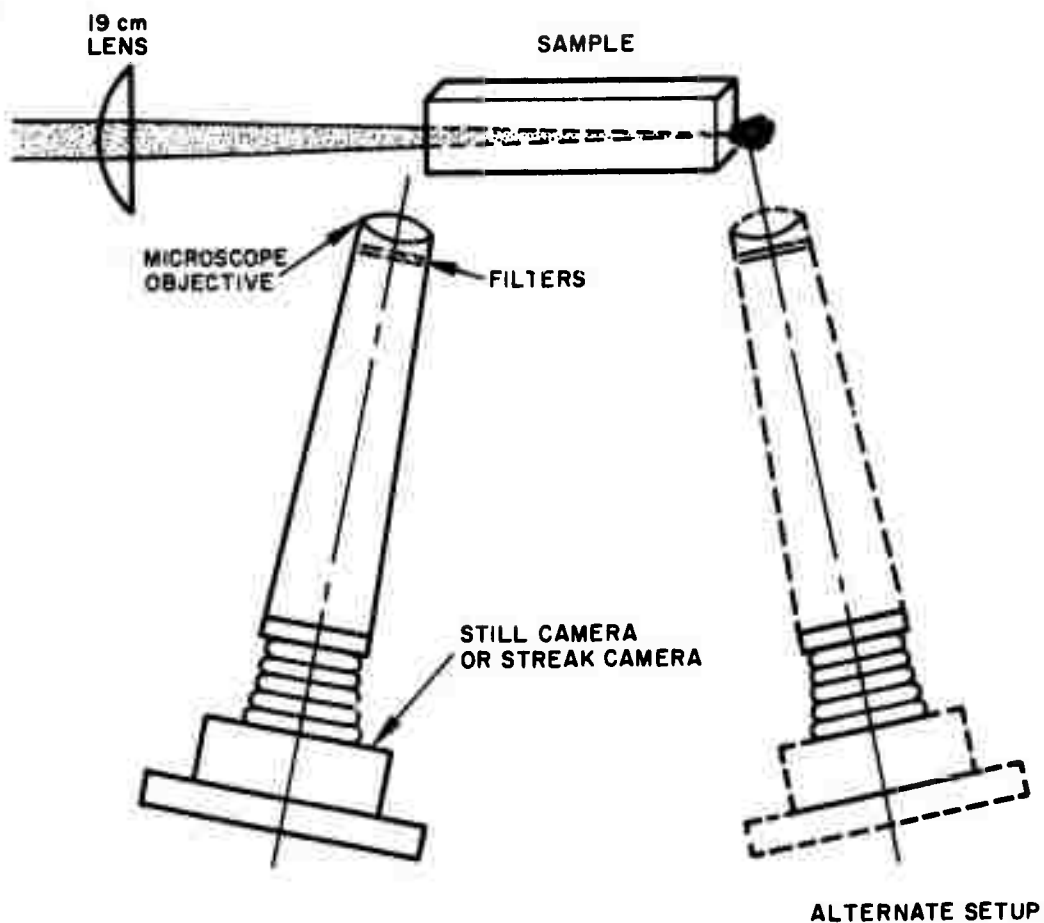


Fig. 5. Schematic diagram showing setup used for photographing surface plasmas both for still and streak photography.

detectable plasma or spark. For example, when the sample was viewed through a Wratten 70 (red) filter, the plasma was not detectable either visually or photographically, whereas the light from the plasma was easily seen through a Corning 4-94 (blue-green) filter, which is a blocking filter for  $6943\text{\AA}$ . A series of experiments was initiated in which the sample was irradiated well above damage threshold and the plasma observed as the power was gradually reduced. During this series the accompanying plasma was seen to decrease in size and brightness as the laser power was reduced, until a power point was reached at which the spark was no longer seen. After laser irradiation in this power regime, a number of micropits were seen on the surface when carefully examined through a microscope with properly chosen illumination. This micropitting, which is seen only very close to threshold, is less extensive than the single fracture crater that occurs more often at slightly higher powers. It should be noted that at the times when no plasma was visible, it was possible to see small amounts of laser light scattered from the tiny surface pits which were formed.

The results of these observations suggest that it is possible to obtain exit surface damage without plasma formation. Of course, the nonobservability of a plasma does not necessarily imply that it is not present, and these results alone do not allow us to form any definite conclusions regarding the connection between the damage and the plasma.

### 3. Time Evolution of Surface Plasmas

One reason for the interest in studying the temporal evolution of the surface plasmas has been to determine the direction of growth of the plasmas relative to the crystal surface, which would lead to a possible explanation of the

differences between exit and entrance surface damage. It was pointed out in earlier reports that the exit surface damage is generally characterized by a kind of crater formation with extensive fracturing while the entrance surface damage is more satisfactorily described as a crazing of the surface where a relatively small amount of material appears to have been removed from the surface. Fersman and Khazov<sup>1</sup> have proposed that the reason for the difference in appearance between entrance and exit surface damage is that the surface plasmas move in an upstream direction as they develop in time. According to their proposed mechanism, the exit plasma grows into the surface causing more extensive damage than the entrance plasma which grows away from the surface. They observe a compressional wave which propagates inwardly from the exit surface and attribute its origin to the interaction of the plasma with the exit surface. Compressional waves arising from damage sites in solids have been observed by others using both schlieren and holographic techniques.<sup>2,3</sup>

We have employed an STL image converter camera operating in the streaking mode for observing the growth of the entrance and exit surface plasmas (see Fig. 5). For these experiments, the unamplified output from our single mode ruby laser was focused with a 19 cm lens on the desired surface of the sapphire sample being examined. Typical laser output is about 20 mJ in a 20 nsec pulse, which gives a power density at the focus of approximately  $10 \text{ GW/cm}^2$ . For the streak camera experiments, a portion of the incident laser light was allowed to enter the camera directly to serve as a marker streak for synchronization purposes.

Streak photographs showing the temporal development of the surface plasmas are shown in Figs. 6 and 7. Essential features of these photographs to be noted are

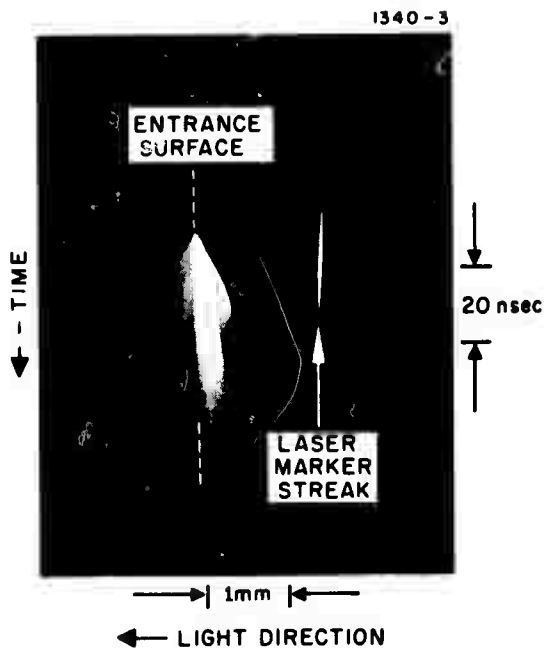
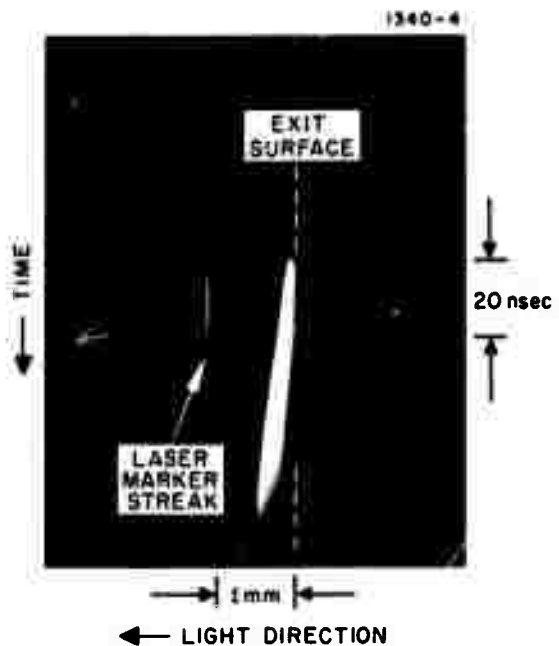


Fig. 6.  
Streak photograph of entrance  
plasma on sapphire surface  
showing two temporal  
components.

Reproduced from  
best available copy.

Fig. 7.  
Streak photograph of exit  
plasma on sapphire surface.





- The plasmas grow away from the surfaces in both cases, the entrance plasma growing in the upstream direction and the exit plasma in the downstream direction
- The entrance plasma has two temporal components whereas the exit plasma has one temporal component
- The extent of growth and luminosity of the faster growing component of the entrance plasma depends on the incident laser pulse in that it ceases to expand and to emit light when the laser terminates
- The slower growing longer lived component of the entrance plasma expands at about the same rate as the exit plasma. These plasmas continue to expand outward and emit light long after the laser has terminated.
- Typical velocities of expansion of the luminous plasma fronts are  $\sim 2 \times 10^6$  cm/sec for the short-lived entrance component and  $\sim 1 \times 10^6$  cm/sec for the long-lived entrance component and the exit plasma.

Several ideas are suggested by these observations.

First, the fact that both entrance and exit plasmas grow away from the surfaces suggests that the mechanism proposed by Fersman and Khazov is incorrect. From the time dependences of the plasmas relative to the incident laser pulse it can be inferred that the short-lived entrance component is a plasma supported in the ambient atmosphere and sustained directly by the laser beam itself, while the longer-lived components at both surfaces result from a kind of micro-explosion caused by the deposition of energy at the surface.

#### 4. Spatial Differentiation of Surface Plasmas

To test these hypotheses further, we devised additional experiments that were designed to allow a spatial differentiation of the plasmas. The reasoning behind these experiments

is as follows. A plasma sustained directly by the light beam would be expected to exist only where the light is present and to be directed along the light beam independent of the angle at which the light enters the material. A plasma which results from a surface explosion caused by a deposition of energy at the surface would be expected to extend in a direction normal to the surface no matter at what angle the light should enter the material.

Figure 8 shows time integrated photographs of the entrance plasma formed when the light is allowed to strike the surface at angles other than normal incidence. The photographs show the separation of the plasma into different spatial components. One component extends along the direction of the light beam; this apparently is the short-lived air plasma. Another component that extends normal to the surface can be seen; this is the component resulting from the surface explosion. A third more diffusely defined plasma component can be seen, extending in the direction of the light reflected from the surface and is presumably additional air plasma sustained by the reflected light. Figure 9 shows a time-integrated photograph of the exit plasma formed when the light leaves at an angle of  $45^\circ$  to the surface. This photograph shows the plasma directed normal to the surface, as expected if a surface explosion were taking place.

As a final confirmation of assignments for the different plasma components, we looked at the entrance plasma in a vacuum. Figure 10 shows photographs of the entrance plasma for a sample tilted  $26^\circ$  from the incident light both at 1 atm pressure and at about 1 Torr pressure. Because of the shape and size of the container, it was impossible to perform the experiment at angles larger than  $26^\circ$ . As a result, the two spatial components are not distinguishable in Fig. 10(a) and (b). However, note that when the air is removed

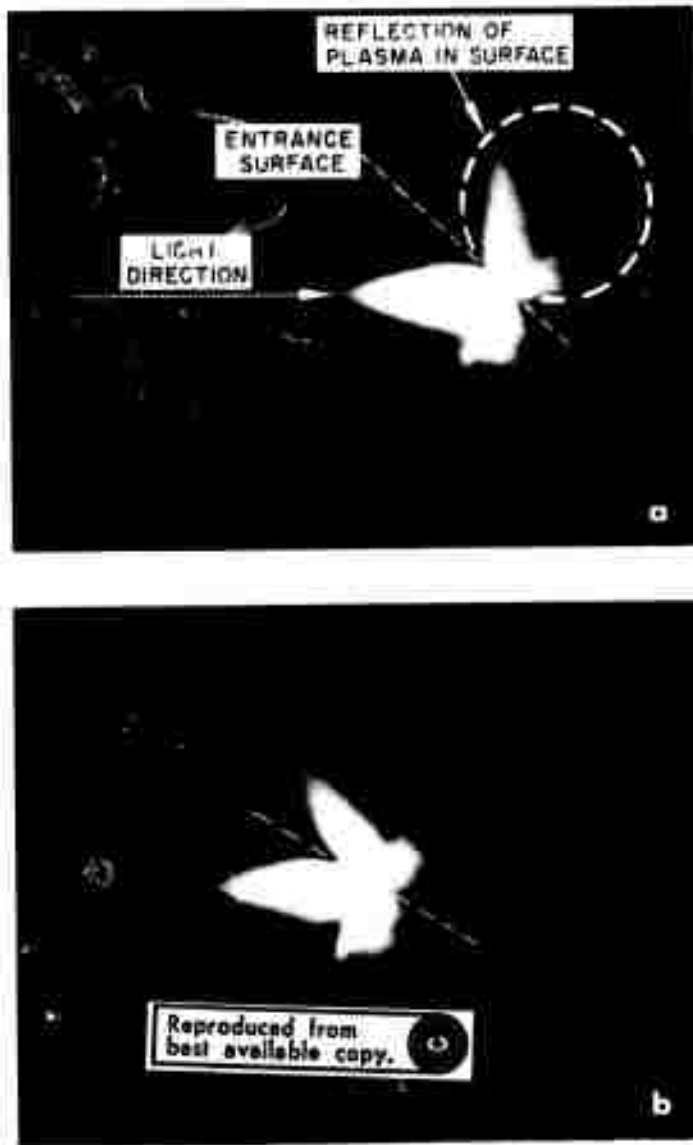


Fig. 8. Time integrated photographs of entrance plasma at sapphire surface tilted with respect to incident beam direction. Angle between light direction and surface normal (a)  $45^\circ$  (b)  $60^\circ$ .

1340-5



Fig. 9.  
Time integrated photograph  
of exit plasma at sapphire  
surface tilted  $45^\circ$  with  
respect to light propagation  
direction.

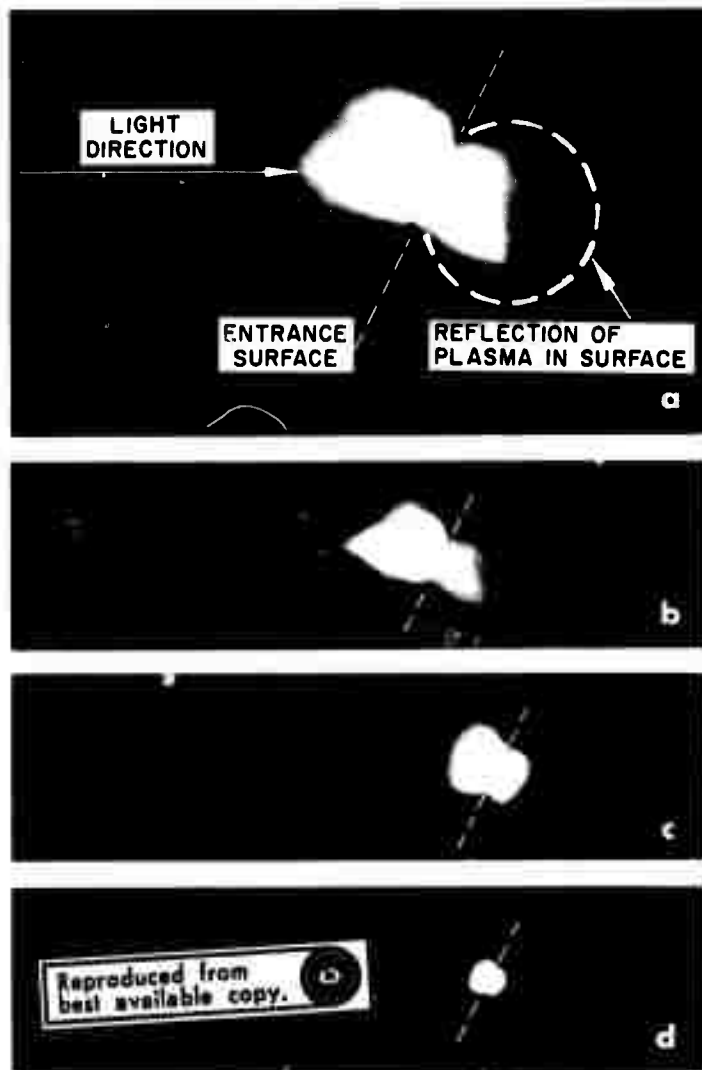


Fig. 10.  
Time integrated photographs of entrance plasma at sapphire surface tilted  $26^\circ$  from beam direction for different optical attenuations at camera. (a) and (b) taken at 1 atm in air, (c) and (d) taken at 1 Torr pressure. Optical attenuation (a) N.D. 1.0 (b) N.D. 1.7 (c) N.D. 0.7 (d) N.D. 1.7.

from the system (Fig. 10(c) and (d)), the plasma component which extends along the light beam is no longer seen; the plasma visible in vacuum is directed normal to the surface, i.e., only the explosion plasma remains.

As a result of these experiments, the following conclusions were reached. First, the surface plasmas are a result rather than a cause of the surface damage. Second, two kinds of plasmas occur at the entrance surface, one which is sustained by the light beam in the ambient atmosphere and another which arises from a microexplosion at or near the surface. The exit surface plasma is of the explosion type. While it may be true that some of the features seen on the surface of a material that has been subjected to damaging laser radiation might be caused by the interaction of the plasma with the surface, the primary cause of the damage is not the plasma. Rather, the surface plasmas are a result of the process or processes, whatever they may be, that affect the surface damage.

It is still not clear why the exit damage is physically so different in appearance than entrance damage. If the mechanism of energy deposition were simply one of surface absorption it would be expected that the damage would be very similar on both surfaces. For some reason, there seems to be a distinct directionality to the surface damage mechanism. Since the exit surface damage threshold appears to be a power density phenomenon (see Section I-B) and since it is not apparently dependent on whether the beam is converging or diverging before it reaches the surface, one would be inclined to conclude that the damage mechanism does not depend strongly- if at all, on phenomena which take place in the bulk of the material. It appears to be strictly a surface or near-surface phenomenon. The possibility that a directed intense acoustic

wave<sup>4</sup> is involved in the damage mechanism is still open, although Stimulated Brillouin Scattering (SBS) is not likely since there seems to be no correlation between SBS thresholds and damage thresholds for a number of different solids. A mechanism of the type proposed by Hellwarth for bulk damage<sup>5</sup> might be a valid surface damage mechanism. The end result of this mechanism is the generation of intense acoustic phonons, but whether one would expect the acoustic wave to be directed in any particular way is not known at this time.

## 5. Spectral Content of Surface Plasmas

The resolution of the entrance plasma into two distinct temporal and spatial components led to the question of whether the spectral content of the air plasma was different from that of the explosion plasma. A number of streak photographs of the entrance plasma viewed through different band-pass filters were taken. For this purpose we used OTI interference filters with transmission maxima ranging from 4040 to 7060 Å; the typical spectral width of these filters is 200 Å (FWHM). The purpose of these qualitative observations was to determine whether a difference exists in the relative amounts of light recorded from the two different entrance plasma components for the different spectral bands employed. Figure 11 shows a number of streak photographs of the entrance plasma viewed through different spectral bands. It is seen that the amount of light from the plasmas drops off significantly above ~5500 Å, very little being detected through the 5790 Å filter and none through the 7060 Å filter. Also, the relative amounts of light from the fast and slow plasma components is essentially the same as viewed in the different spectral regions. A similar set of experiments on the exit plasma yielded similar results.

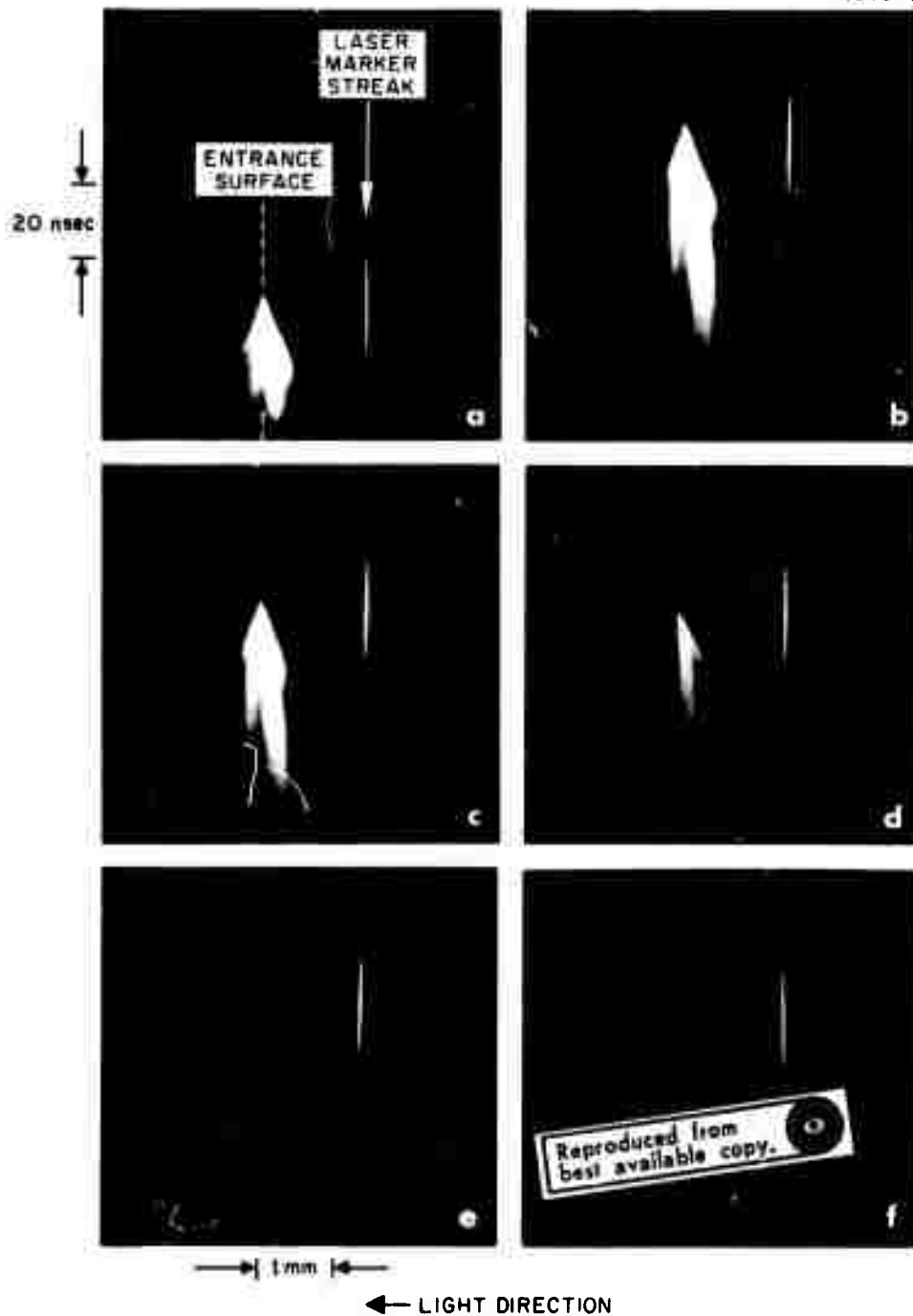


Fig. 11. Streak photographs of entrance plasma as viewed through different interference filters (FWHM  $\sim 200$  Å). Peak wavelength of filters is (a) 4040 Å, (b) 4230 Å, (c) 4360 Å, (d) 5460 Å, (e) 5790 Å.



While these observations indicate that the two entrance plasma components are spectrally similar, it does not necessarily mean that they are the same. The results of early spectroscopic measurements performed at HRL<sup>4</sup> on a number of different materials showed that the light emitted from the exit plasmas contained spectral lines characteristic of the materials being irradiated. Presumably, the entrance plasma is both an air plasma and a material plasma and would probably show spectral lines characteristic of both the material and of the ambient atmosphere. Detailed spectroscopic investigations of both types of plasma would certainly yield a definitive assignment, but at this time we are confident from the results presented earlier in this section that the nature of the plasmas is understood.

#### D. THE EFFECT OF ION BEAM POLISHING ON SURFACE DAMAGE

A few experiments have been performed, which were designed to determine whether it might be possible to improve the surface damage resistance of materials by improving the quality of the surface finish. One such method of obtaining surfaces free of scratches and other influences of mechanical damage arising from conventional abrasive polishing is the use of ion beam sputtering. This technique employs a beam of energetic ions ( $\text{Ar}^+$  in this case) that are made to impinge on the surface at an angle of  $\sim 20^\circ$  from grazing incidence. The effect is to remove material from the surface in a manner very different from that in abrasive polishing. Experiments performed at HRL, in conjunction with the Ceramic Section of the Naval Research Laboratory, have indicated that this microsmoothing technique increases the tensile strength of materials such as sapphire, spinel, and magnesium oxide by as much as a factor of 10.

The first ion polished sapphire sample was sample L134, a Union Carbide sapphire bar, the exit surface damage threshold of which had been measured extensively for a wide range of spot sizes and beam divergences (see Section I-B). Here the exit surface damage threshold for the surface before ion polishing was found to be  $1 \text{ GW/cm}^2$ . After being subjected to the ion beam at a nominal exposure (4 kV and  $300 \text{ } \mu\text{A/cm}^2$  for one hour) the exit damage threshold in parts of the surface that had not previously been irradiated with the laser was remeasured. A typical set of experiments involves focusing the beam on a particular spot on the surface and firing the laser for a series of shots of increasing power until damage threshold is reached. Then the sample is moved, and a different spot is subjected to another series of shots. The results of the first set of experiments on the ion polished sample are given in Table I. The table data indicate from these early results that the surface was subjected to power densities substantially higher than the previously determined threshold of  $1 \text{ GW/cm}^2$  without being damaged. The highest power density in which damage was not produced was shot 14 at  $4.34 \text{ GW/cm}^2$  while the lowest value where damage was obtained was shot 11 at  $3.0 \text{ GW/cm}^2$ .

The sample was then "cleaned" with ethyl alcohol and water to see if this would affect the surface threshold. A series of 28 shots over 16 different surface locations showed a wide variation of powers where damage was obtained. The highest power for which no damage occurred was  $4.7 \text{ GW/cm}^2$ , while the lowest power for which damage did occur was  $0.9 \text{ GW/cm}^2$ . Since high powers without damage were still observed, it was felt that the wide variation was due to the possibility that the extent of ion polishing was not sufficient to remove all the scratches and other influences of mechanical damage from the abrasive polishing.

TABLE I

Exit Surface Damage Data on Sapphire Sample L134  
after Ion Beam Polishing

Shot No.	Beam Coordinate on Surface, (x,y) mm	Power Density GW/cm <sup>2</sup>	Observation
1	4.5,5	0.97	No damage
2	4.5,5	2.97	No damage
3	4.5,5	5.09	Damage Crater
4	4.5,5.5	1.05	No damage
5	4.5,5.5	1.65	No damage
6	4.5,5.5	2.62	No damage
7	4.5,5.5	3.03	No damage
8	4.5,5.5	3.21	No damage
9	4.5,5.5	3.62	No damage
10	4.5,5.5	4.17	Damage crater
11	4.5,5.3	3.00	Damage crater
12	4.5,6	3.43	No damage
13	4.5,6	3.29	No damage
14	4.5,6	4.34	No damage
15	4.5,6	6.09	Damage crater

T358

Another sapphire sample, L132, was subjected to threshold measurements. The results of eight shots on six locations gave a threshold of  $0.9 \text{ GW/cm}^2$  before ion beam polishing. After ion beam polishing, a series of 28 shots on ten different locations again gave a wide range of values. Certain spots sustained power densities as high as  $7 \text{ GW/cm}^2$  without damage, while others were damaged at  $1 \text{ GW/cm}^2$ .

The wide variation in threshold for the ion polished surfaces compared with the standard mechanically polished surfaces suggests that certain regions are being strengthened considerably by the ion polishing but that others are still unchanged. Microscopic examination of the surface after ion polishing showed that some scratches remained, although no correlation existed between the location of the scratches and the more easily damaged regions.

At this point in the investigation, the results seem to indicate that ion beam polishing has a definite effect in substantially increasing the surface damage threshold in sapphire. The wide variation in threshold from place to place is not understood, but it may be a result of a residual influence of mechanical polishing. Another observation to be noted here is that the damage when it occurs at these higher thresholds is considerably more extensive than the damage at the lower thresholds, the craters being larger and more extensively fractured. This seems to suggest that the mechanism for the deposition of energy in the surface is probably not affected much by the ion polishing but the surface strength is increased. Hence the surface seems to be behaving as a stronger "container" for the subsurface pressures, which are allowed to build up to a higher value before rupture occurs. However, when breakdown occurs, it is more catastrophic as a result of having been contained longer.

At this time we have not had an opportunity to systematically vary the parameters and conditions of the ion beam polishing process, nor has any detailed characterization of surface quality been attempted, except for microscopic examination. Now that we have an indication of the potential of this technique for increasing the surface damage threshold we will continue to explore the phenomenon more systematically during the next period.

#### E. BULK DAMAGE AND SELF-FOCUSING FOR NONCIRCULAR BEAMS

The last report discussed some results of experiments in which an attempt was made to generate internal damage in sapphire using cylindrical lenses for focusing inside the sample. Experiments failed to obtain damage at power densities ten times higher than that previously obtained with circular spots of the same area. This led us to suspect that self-focusing might be sensitive to beam shape. If one considers an elliptically shaped beam of constant intensity entering a medium having an index nonlinearity  $\Delta n$  proportional to power density and define the critical power  $P_c$  to be that for which the angle for total internal reflection at the boundary equals the far-field diffraction angle characteristic of the smaller beam dimension, we find that the critical power increases linearly with the beam aspect ratio  $a/b$ , where  $a$  and  $b$  are the long and short dimensions of the elliptical beam. The critical angle for total internal reflection is given by

$$\cos \theta_c = \frac{1}{1 + \Delta n/n} \quad (1)$$

If we expand the cosine for small angles and the right-hand side of eq. (1) for small  $\Delta n/n$ , we obtain

$$1 - \theta_c^2/2 = 1 - \Delta n/n , \quad (2)$$

and

$$\theta_c^2 = 2\Delta n/n = KP_c/\pi ab , \quad (3)$$

where  $K$  is a product of constants whose value depends on the choice of units.

The diffraction angle characteristic of the smaller dimension  $b$  is

$$\theta_{\text{diff}}^2 \sim \lambda^2/b^2 . \quad (4)$$

When the two angles are set equal

$$P_c = K'\lambda^2(ab/b^2) = P_c^\circ(a/b) , \quad (5)$$

results, where  $P_c^\circ$  is the critical power for a circular beam ( $a = b$ ). The diffraction criterion for the small beam dimension was chosen because it assured that the turning in of the rays would be accomplished for the whole beam under those conditions. It can be seen that at a lower power  $P_c' = P_c^\circ(b/a)$ , there will be a sufficient nonlinearity for overcoming diffraction in the direction of the long dimension but the remainder of the beam will continue to diffract.

Recently, A. Yariv of California Institute of Technology and J. Marburger of University of Southern California have become interested in this phenomenon. Their separate approaches differ somewhat, but both are based on a more rigorous treatment of the nonlinear wave equation and each predicts the same dependence on aspect ratio as eq. (5) in the limit of large aspect ratio.

Additional experiments were performed in which a spherical and a cylindrical lens combination was used to obtain damage threshold power for circular beams of different sizes compared with elliptical beams. The first three entries in Table II show the damage threshold power for circular beams of different sizes obtained from earlier measurements. As pointed out in previous reports, there is not a constant power threshold because the influence of electrostriction makes it more difficult to reach self-focusing threshold with large beams than with small beams. The beam dimensions listed in the table are those at the beam waist where the self-focus first forms at threshold. The remaining entries in Table II show the effect of noncircular beam shapes. The fourth entry gives the threshold power for an elliptical beam whose short dimension is the same as the first entry, whose long dimension is the same as the third entry, and whose area is the same as the second entry. We see that the threshold power is appreciably higher for the elliptical beam compared with any of the circular beams. The last two entries in Table II show data for more elongated elliptical beams where we were unable to reach threshold at the maximum power available from our system. The elliptical beam profiles were measured using the multiple lens camera setup described in Semiannual Report 3.

The implications of these results are very important. They indicate that any difficulties with high power light beams (whether with damage or merely propagation) which arise from self-focusing can be avoided by selecting the appropriate beam shape.

TABLE II

Damage Threshold in Sapphire for Different Beam Shapes

Beam Radii at Waist, <sup>a</sup> $\mu\text{m}$	Beam Area at Waist, $\mu\text{m}^2$	Threshold Power, MW
Circular ( $a/b = 1$ )		
20	$12.6 \times 10^2$	0.51
53	$88 \times 10^2$	0.79
140	$615 \times 10^2$	1.23
Elliptical		
20 x 140 ( $a/b = 7$ )	$88 \times 10^2$	4.5
20 x 1700 ( $a/b = 85$ )	$1070 \times 10^2$	$> 17^b$
10 x 1700 ( $a/b = 170$ )	$540 \times 10^2$	$> 17^b$
<sup>a</sup> Beam radius is defined as the $1/e^2$ radius for intensity. <sup>b</sup> Unable to reach damage threshold at this power.		

T359

A detailed appreciation of self-focusing with noncircular beams has yet to be obtained. Detailed calculations of the on-axis intensity as a function of incident power and beam shape parameters will shed more light on the dynamics of the phenomenon. It may prove that different parts of the beam (i.e., rays having different characteristic diffraction angles) will tend to self-focus with different characteristic self-focusing distances, which would indicate that the on-axis intensity may never reach a high value. More work on this very interesting phenomenon will continue during the next period.



## SECTION II

### THEORETICAL STUDIES ON OPTICAL DAMAGE

During this reporting period, emphasis was concentrated on two main areas: (1) the question of whether optical breakdown does or does not involve an avalanche of hot (i.e., ionizing) electrons, and (2) how to measure the surface absorption at faces of laser crystals so that the role of this absorption in surface damage may be assessed. A summary of the progress in these two areas follows. A brief account of other areas believed to deserve further study in understanding optical damage is also given.

#### A. MECHANISMS OF OPTICAL BREAKDOWN

At the time this project began, the existing theories of optical breakdown in ideal crystals all hypothesized the creation by the high optical electrical fields of enough "hot" electrons (of ionizing energy) to create an ionizing avalanche. In the first semiannual report of this project, it was shown, using the same "Frölich" model for a conduction electron in a polar lattice from which other theories had started, that the average kinetic energy of such an electron would not be significantly above  $kT$  (the lattice temperature times Boltzmann's constant) in the optical fields at which breakdown was believed to occur. However, as was stated there, "A possible complication that we will study further is that a very few electrons might be created in the high-energy wings of the electron distribution."

In our fourth semiannual report, the equations were developed which determine the electron energy distribution and, after several simplifying assumptions, it proved possible to cast them in a form that might be solved on a computer. However, we have not expended the considerable effort that would be required to do this; efforts to see analytically whether a high energy tail would be predicted in the electron distribution have not proved fruitful.

In conclusion, we do know that potentially damaging amounts of heat ( $\sim 10^2$  J/cm<sup>-3</sup>) will be transmitted from the optical beam to the lattice by cold electrons at optical intensities around  $10^{10}$  to  $10^{11}$  W/cm<sup>2</sup> if the light has created at least  $10^{16}$  photoelectrons/cm<sup>3</sup>. This was demonstrated in Semiannual Report 2 (and reported at the Second Annual Symposium on Laser Damage, Boulder, Colorado, June 1970). However, it is not known whether the crystal in fact holds together until self-focusing produces high enough intensities to heat the electrons to ionizing energies.

Semiannual Report 4 documented the first conclusive experimental evidence that self-focusing had actually been occurring whenever bulk damage was produced in ruby or sapphire. Whenever self-focusing sets the threshold for damage, it is much less interesting to know what is the actual mechanism of rupture; consequently, high priority has not been given to determining at what optical intensity hot electrons should become numerous. However, this mechanism may yet be important in understanding surface damage, and so the issue may regain importance.

## B. MEANS OF MEASURING SURFACE ABSORPTION

As experimental efforts in this project have shifted from studying bulk damage to studying surface damage, the theoretical study of possible mechanisms of surface damage has been initiated. For the nanosecond to picosecond optical pulses under consideration, localized surface heating would have no time to diffuse during the pulse, and a small fractional surface absorption could produce enormous thermal gradients and high surface temperatures. Therefore, our first efforts have been concentrated on finding ways to measure the amount of surface absorption and the depth of the absorption layer. Once these are known, it is simple to estimate whether the surface absorption at damage threshold could be responsible for the damage and also the feeding (by evaporation) of the observed plasma plumes.

### 1. Measurement by Temperature Rise

Assuming there exists an absorbing layer, much thinner than a wavelength, on a crystal's surfaces, then if the path length being traversed through the crystal by the optical beam is short enough, most of the heating will arise from the surface absorption. From the specific heat of sapphire, it is estimated that if 1% of an optical pulse were absorbed by a  $10^{-2}$  cm thick slab of sapphire, a temperature rise of about  $1/3^{\circ}\text{C}$  would be created by each Joule per  $\text{cm}^2$  in the incident pulse. It can also be estimated that for temperature rises less than several degrees, the cooling of the slab would be mainly by convection in air and would have a time constant of a few seconds, enough time to observe the temperature rise with, for example, a thermocouple.

One can also extrapolate from these figures, assuming a temperature-independent specific heat, that if a 1% absorbing layer existed that was 1000 Å thick, a nominal  $10 \text{ J/cm}^2$  short optical pulse would produce a catastrophic temperature rise, of order  $10^4 \text{ K}$ . This temperature would scale inversely with layer thickness and in an obvious way with the other parameters.

## 2. Measurement by Altered Dielectric Reflection and/or Transmission

It is a straightforward matter to derive the reflection and transmission of a plane wave incident through a lossless medium (of dielectric constant  $\epsilon = n^2$ ) and at angle  $\theta$  to the normal, upon a uniform absorbing layer, of complex dielectric constant  $\epsilon_\ell$  and thickness  $\ell$ , that is followed by a lossless semi-infinite crystal medium having a real dielectric constant  $\epsilon_c$ . The results show, for example, that at normal incidence there will be a change  $\delta R$  in the reflectivity  $R$  (from the case of no absorbing layer), if  $\delta R \ll R$ , of

$$\delta R/R = -4(\omega\ell/nc)(1 - \epsilon_c/\epsilon)^{-1} \text{Im } \epsilon_\ell, \quad (6)$$

where  $\omega$  is the optical (angular) frequency. The fraction of the incident beam absorbed in the layer is

$$-(\delta R/R)(1 - \epsilon_c/\epsilon)/(1 + \epsilon_c/\epsilon)$$

and is seen to be of order  $1/2(\delta R/R)$  for sapphire. It is difficult, though possible, to see a percent deviation in reflectivity from nominal; thus reflectivity measurements are a feasible way to measure the layer absorption. (The fractional change in transmission is generally much smaller and more difficult to interpret because it must involve two crystal surfaces.)

Two improvements over the straightforward foregoing measurement suggest themselves. First, one might vary the index of the incident medium (by placing the crystal in a liquid of variable composition) in contact with the surface of the crystal. As the nominal reflection passed through zero ( $\epsilon = \epsilon_c$ ), the actual residual reflection due to the layer would be (at  $\theta = 0$ )

$$(\omega \ell / nc)^2 |\epsilon_\ell - \epsilon|^2 / 4, \quad (7)$$

which is roughly the square of the fraction absorbed. Though small, this reflection might be measurable (with some complications from birefringence) because there is little "normal" background reflection.

A second improvement might be to measure the residual reflection of the nominally unreflected polarization at Brewster's angle. Rather than vary the incident medium index, one could plot this reflection versus angle of incidence and polarization near Brewster's angle to discern the small residual reflection, which again would be of the order the square of the fraction absorbed in the beam.

The main advantage of the reflection measurements over the temperature change measurements is that, although they may be more difficult, they offer the possibility of determining the layer thickness by comparing reflectivities at enough different angles and polarizations so that  $\text{Re } \epsilon_\ell$ ,  $\text{Im } \epsilon_\ell$ , and  $\ell$  can all be solved for through the theoretical expressions. The fact that an absorbing layer might not be uniform up to depth  $\ell$  would complicate this determination, though not impossibly.

### SECTION III

#### PLANS FOR NEXT PERIOD

During the next period we will continue to pursue the effects of ion beam polishing on surface damage threshold. Studies of surface quality as a function of polishing parameters will be carried out concurrently with the damage measurements. For this purpose we will use the method of Berg-Barrett x-ray diffraction topography and high resolution optical and scanning electron microscopy. We will also obtain further experimental data on self-focusing with elliptical beams in an attempt to obtain a more quantitative measure of the dependence of threshold on beam shape.

In connection with surface damage, it is planned to investigate (1) the creation of photoelectrons from surface states and the measurement of surface photoconductivity. Such photoelectrons could play a similar role in surface damage as has been proposed for them in bulk damage; (2) the determination of the energy in the observed plasma shock front that is formed during surface damage; and (3) methods for determining how much crystal is evaporated during surface damage.

**Preceding page blank**

#### REFERENCES

1. I.A. Fersman and L.D. Khazov, Sov. Phys.-Tech. Phys. 15, 834 (1970).
2. T.P. Belikova, A.N. Savchenko, and E.A. Sviridenkov, Sov. Phys. JETP 27, 19 (1963).
3. N.L. Boling and R.W. Beck, "Damage in Laser Materials: 1971," A.J. Glass and A.H. Guenther, Eds., Nat. Bureau of Standards Special Publication 356 (Nov. 1971).
4. C.R. Giuliano, Appl. Phys. Letters 5, 137 (1964).
5. R.W. Hellwarth, "Damage in Laser Materials," A.J. Glass and A.H. Guenther, Eds., Nat. Bureau of Standards Special Publication 341 (Dec. 1970). (See also HRL Semiannual Technical Report 3, AFCRL-71-0064, January 1971.)